Multi-physics Simulation of a Circular-Planar Anode-Supported Solid Oxide Fuel Cell

Keyvan Daneshvar[*1], Alessandro Fantino[1], Cinzia Cristiani[1], Giovanni Dotelli[1], Renato Pelosato[1], Massimo Santarelli[2]
[1]Politecnico di Milano, Dipartimento di Chimica, Materiali e Ingegneria Chimica "G. Natta", Milano, Italy
[2]Politecnico di Torino, Dipartimento di Energetica, Torino, Italy
*Corresponding author: keyvan.daneshvar@mail.polimi.it

Abstract: In this paper a 2D isothermal axisymmetric model of an anode-supported Solid Oxide Fuel Cell (SOFC) has been developed. This model has the advantage of being able to work with different operating parameters: the results shown here are based on a temperature of 1073 K, a pressure of 1 atm and Ni-YSZ/YSZ/LSM-YSZ as materials for the anode, electrolyte and cathode respectively. Among the results of the simulation process, the most important ones are polarization and power density curves that showed a good agreement with the experimental data, then the profiles of cell potential, electrolyte current density, mass fractions, velocity and pressure, and finally the parametric curves. Future improvements are planned in both the geometry (transition to more comprehensive one) and analysis (i.e. heat profile).

Keywords: Solid Oxide Fuel Cell, SOFC modeling, Parametric Study.

1. Introduction

Solid Oxide Fuel Cells represent a promising technology due to their high efficiency, long-term stability, fuel flexibility, and near-to-zero carbon emissions compared to the other power sources. Research in this field, including computational modeling, in order to expand the potential and reduce the disadvantages plays an important role in the affirmation of this technology as a viable energy alternative.

SOFCs are characterized by a solid oxide electrolyte to conduct negative oxygen ions from the cathode to the anode: the most used material is the yttria stabilized zirconia (YSZ). Also the electrodes are made with solid oxides: the anode, where the electrochemical oxidation of the hydrogen occurs, is a cermet made up of nickel mixed with YSZ (Ni-YSZ), while the cathode, where oxygen reduction takes place, is a composite of lanthanum strontium manganite (LSM) and YSZ. These materials have been chosen also for the model. Another specific feature of SOFCs compared to other types of cells is the high working temperature, typically between 800 to 1000 °C: this represents the largest disadvantage, due to increasing costs and longer start-up times, but in this way SOFCs do not require such an expensive platinum catalyst material, as is currently necessary for lower temperature fuel cells. Also with using new kind of electrolytes the working temperature of SOFCs could be decreased between 600 and 800 °C to have less disadvantages in comparison with high temperature one. SOFCs could have different geometries. Laboratory scale experiments usually adopt anode-supported button cell: the origin of the name derived from the fact that the anode, the electrolyte and the cathode are stacked one above the other in the form of thin disks. "Anode-supported" because the anode is the thickest and strongest layer placed on the bottom of the cell, providing the mechanical support [1-3].

2. Model Description

The geometry of the model is illustrated in Figure 1: it is an axisymmetric geometry, so it means that, applying a revolution through the axis of symmetry, a 3D geometry is obtained. This choice has been taken to reduce the calculation time, shorter than 3D geometry. The radius of the cell is 40 mm, while the thickness of the anode, electrolyte and cathode are respectively 540, 6 and 36 μm. The geometry of feeding system is the same for both the fuel and the oxidant and each one is composed by two concentric channels, one inside the other: hydrogen and air enter from the inner channel, and the species do not diffuse and the reaction products come out through the outer channel. The radius of the inner channel is 14 mm with a

thickness of 2 mm. The distance between the channels and the reference electrodes" standoff distance" is 20 mm. After the geometry building, it's then necessary to decide which mathematical approaches should be used. In particular, for this work these kinds of SOFC modeling have been chosen:

1. Ohm's law for the electronic and ionic charge balance.
2. Butler-Volmer kinetics for the charge transfer.
3. Navier-Stokes equations for the flow distribution in the gas channels.
4. Brinkman equations for the flow in the porous gas distribution electrodes.
5. Maxwell-Stefan diffusion and convection for the mass balances in gas phase in both gas channels and porous electrodes.

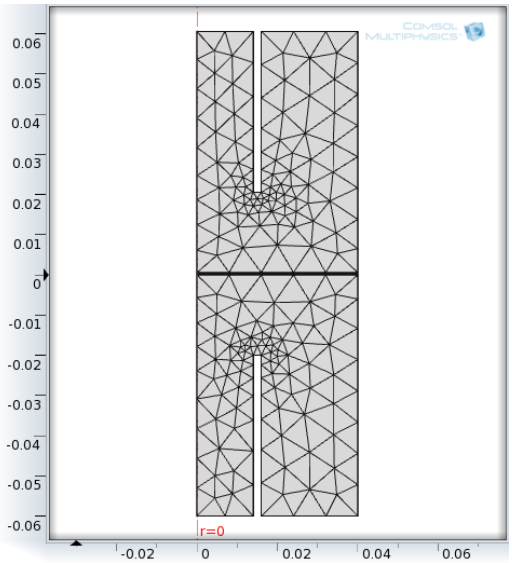

Figure1. Axisymmetric meshed geometry of the setup

In order to simplify the computation, several assumptions are considered and applied:

1.The fuel cell operates under steady-state conditions.
2. Reactant species are compressible ideal gases, completely saturated with water vapor.
3.The flow of the species is laminar.
4.The electrolyte is impermeable to reactant gases, only oxygen ions pass.
5. Materials are isotropic and homogenous, their chemical and physical properties are constant in time with no degradation [4-9].

3. Use of COMSOL Multiphysics

COMSOL Multi-physics 4.2 was used to design the geometry of the model and to solve it. COMSOL is structured with the variety of interfaces which each of them performs and solves a different physics. In particular, for this model these features were used:

1. The Secondary Current Distribution interface for the electronic and ionic charge balance in the anode, electrolyte and cathode.
2. Transport of Concentrated Species interface for the diffusion in the electrodes and their respective feeders.
3. Free and Porous Media Flow interface for the velocity and pressure fields linked to the species.

Free triangular mesh has been used for the fuel and air channels, while mapped mesh has been used for the cell so as to ensure a good accuracy of the results. The model has been solved using a MUMPS solver across a range of the polarization curve from 0 to 0.53 volt with a study step of 0.01.

4. Governing Equations

The charge balance, studied in the Secondary Current Distribution interface, is based on Ohm's law. The general equation is according to the following [10-13]:

$$\nabla \cdot \mathbf{i}_k = Q_k$$

And (1)

$$\mathbf{i}_k = -\sigma_k \nabla \phi_k$$

Q_k is a generic source term where k denotes an index that is l for the electrolyte or s for the electrode, σ_k is the conductivity (S/m) and ϕ_k the potential (V).

To describe the charge transfer current density the Butler-Volmer formula has been used. At the anode, hydrogen is reduced to produce water; assuming that the transfer of the first electron is the rate determining step, the charge transfer kinetics equation is:

$$i_a = i_{0,a}\left[\frac{c_{h2}}{c_{h2,\,ref}}\exp\left(\frac{0.5F}{RT}\eta\right) - \frac{c_{h2o}}{c_{h2o,\,ref}}\exp\left(\frac{-1.5F}{RT}\eta\right)\right] \quad (2)$$

where $i_{0,a}$ is the anode exchange current density (A/m^2), c_{h2} is the molar concentration of hydrogen (mol/m^3) and c_{h2o} is the molar concentration of water (mol/m^3). $c_{h2,ref}$ and $c_{h2o,ref}$ are the reference concentrations (mol/m^3). F is Faraday's constant (C/mol), R the gas constant (J/mol·K), T the temperature (K), and η the overvoltage (V).

At the cathode, where oxygen acquires two electrons, the charge transfer kinetics equation is:

$$i_{c,} = i_{0,c}\left[\exp\left(\frac{3.5F}{RT}\eta\right) - x_{o2}\frac{c_t}{c_{o2,ref}}\exp\left(\frac{-0.5F}{RT}\eta\right)\right] \quad (3)$$

where $i_{0,c}$ is the cathode exchange current density (A/m^2), $c_{o2,ref}$ is the reference concentration of oxygen (mol/m^3), c_t is the total concentration of species (mol/m^3) and x_{o2} is the molar fraction of oxygen.

Transport of Concentrated Species interface is described by the Maxwell-Stefan equation:

$$\rho\frac{\partial}{\partial t}(\omega_i) + \rho(\mathbf{u}\cdot\nabla)\omega_i = \nabla\cdot\left(\rho\omega_i\sum_{k=1}^{Q}\tilde{D}_{ik}\mathbf{d}_k + D_i^T\frac{\nabla T}{T}\right) + R_i \quad (4)$$

where ρ denotes the mixture density (kg/m^3) and **u** is the mass average velocity of the mixture (m/s). D_{ik} is the multicomponent Fick diffusion coefficient of species i and k (m^2/s) and D_i^T is the thermal diffusion coefficient (kg/m·s). R_i is the rate expression describing production or consumption of the species. $\mathbf{d}_k$ is the diffusional driving force acting on species k, equal to:

$$\mathbf{d}_k = \nabla x_k + \frac{1}{p}\left[(x_k-\omega_k)\nabla p - \rho\omega_k\mathbf{g}_k + \omega_k\sum_{l=1}^{Q}\rho\omega_l\mathbf{g}_l\right]$$

The molar fraction x_k is : (5)

$$x_k = \frac{\omega_k}{M_k}M$$

And the mean molar mass M (kg/mol) is:

$$\frac{1}{M} = \sum_{i=1}^{Q}\frac{\omega_i}{M_i}$$

The flow in the channels, described in the Free and Porous Media Flow interface, is governed by the Navier-Stokes equations:

$$\rho(\mathbf{u}\cdot\nabla)\mathbf{u} = \nabla\cdot\left[-p\mathbf{I} + \mu\left(\nabla\mathbf{u} + (\nabla\mathbf{u})^T\right) - \frac{2}{3}(\nabla\cdot\mathbf{u})\mathbf{I}\right]$$

And (6)

$$\nabla\cdot(\rho\mathbf{u}) = 0$$

where **u** is the gas velocity (m/s), ρ is the gas density (kg/m^3), p is the pressure (Pa) and μ is the gas dynamic viscosity (kg/m·s).

In the porous gas diffusion catalyst layers, the equation changes in:

$$\left(\frac{\mu}{\kappa} + Q\right)\mathbf{u} = \nabla\cdot\left[-p\mathbf{I} + \frac{\mu}{\varepsilon}\left(\nabla\mathbf{u} + (\nabla\mathbf{u})^T\right) - \frac{2}{3}(\nabla\cdot\mathbf{u})\mathbf{I}\right]$$

And (7)

$$\nabla\cdot(\rho\mathbf{u}) = Q$$

where ε is the porosity of the layer and k is its permeability (m^2).

5. Results

Figure 2 shows the polarization curve and the power density vs current density curve obtained from both the experimental data [7,14] and the modeling one: the curves are superimposable, thus confirming the validity of the model.

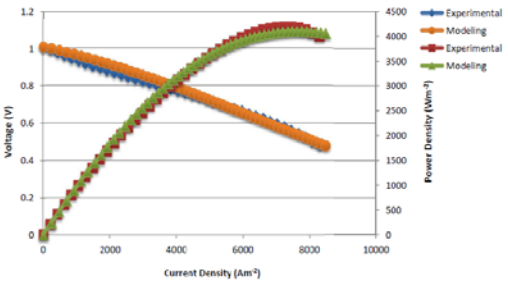

Figure 2. Polarization and power density vs current density curves

Figure 3 and 4 show the trend of the cell potential: the first one illustrates the inside potential of an enlarged section of the cell, whose reference length (the abscissa) is equal to 4 mm. The left edge of the graph is equivalent to the center of the cell. In agreement with the input parameters, the potential at the anode is uniform and equal to zero outside the active area. Inside the active area, the potential taken as an absolute value, increases approximately in a linear manner along the thickness direction. The second one shows the potential on the contact surface between electrolyte and cathode: it is possible to note how in absolute values, the potential decreases approaching the side edges of the cell.

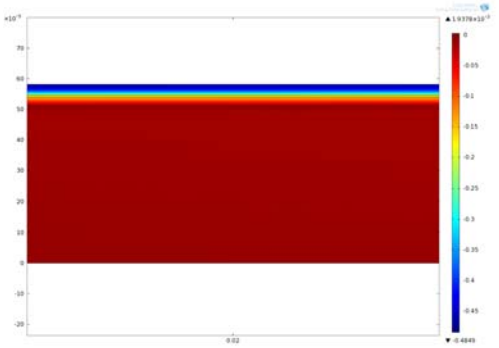

Figure 3. Side view of the cell potential

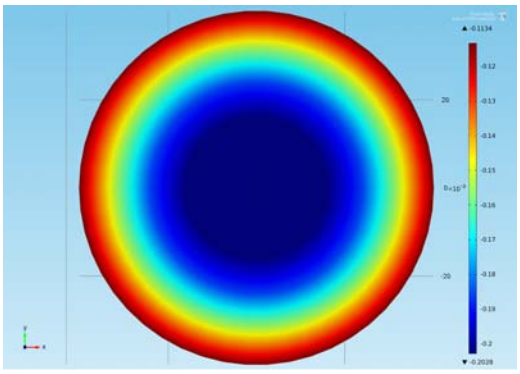

Figure 4. Top view of the cell potential

Figure 5 shows the current density on the contact surface between electrolyte and cathode: it is easily identifiable as it decreases moving away from the center, passing from a value of 14500 A/m^2 to reach a value of about 7300 A/m^2 in the side edges of the SOFC. This variability is attributable to the difference in concentration of the reactant species inside the cell, as shown in the next subsection.

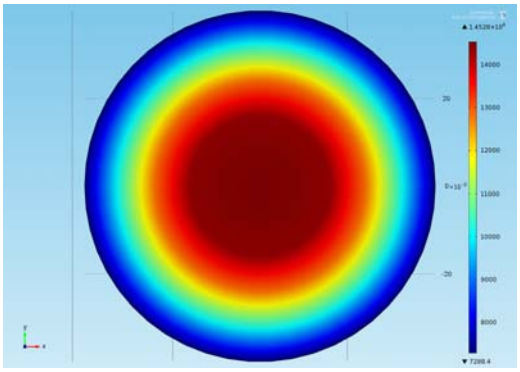

Figure 5. Electrolyte current density

Figures 6, 7 and 8 show the mass fractions of the present species, respectively the mass fraction of the oxygen in the cathodic area and the mass fractions of the hydrogen and the water in the anodic area. For the first two, whose input values are 0.15 and 0.40, it is possible to see how the mass fraction decreases significantly in the edges of the cell due to the difficulty of the species to reach these points, influencing also the current density obtained. The water instead, showed a trend approximately inverse.

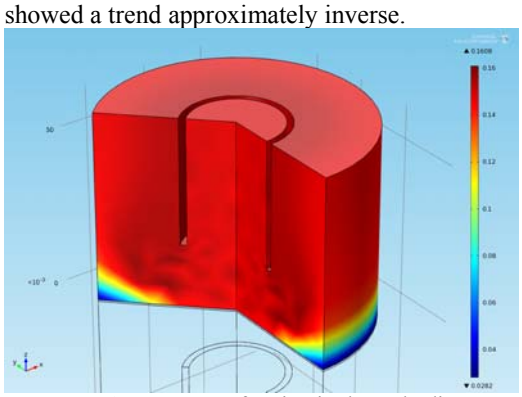

Figure 6. Oxygen mass fraction in the cathodic area

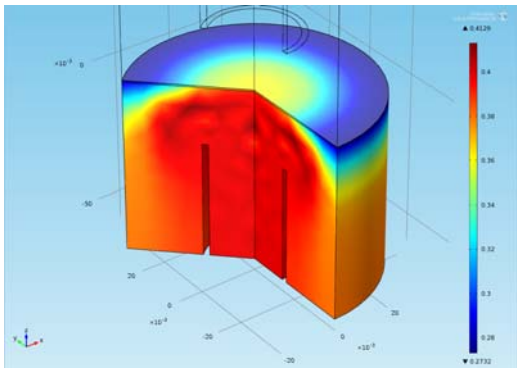

Figure 7. Hydrogen mass fraction in the anodic area

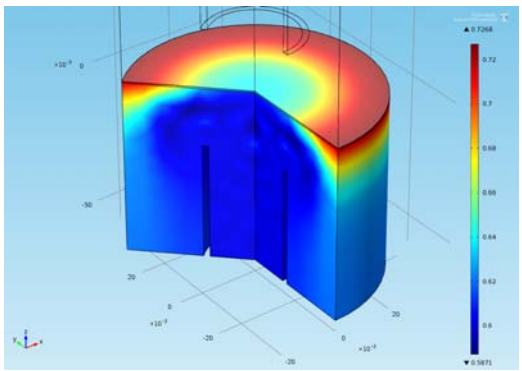

Figure 8. Water mass fraction in the anodic area

Figures 9 and 10 show the velocity and the pressure profiles. The velocity is greater from the inlet to the cell, about 12 m/s, where the way is linear and there's no obstacle to the flow, then it drops dramatically (0.1m/s) due to the absorption of species inside the electrodes. Near the walls, the speed is lower due to friction. The pressure gradient, equal to 2 Pa in the anodic inlet and 6 Pa in the cathodic inlet, is approximately constant in the channels, while greatly increases within the cell arriving up to 15 Pa.

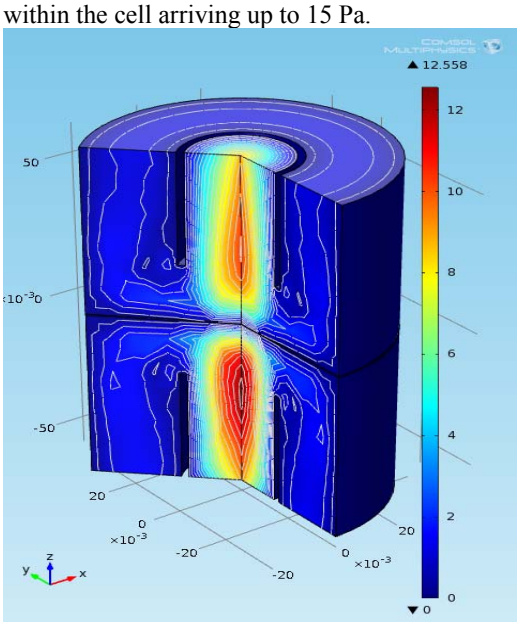

Figure 9. Velocity profile

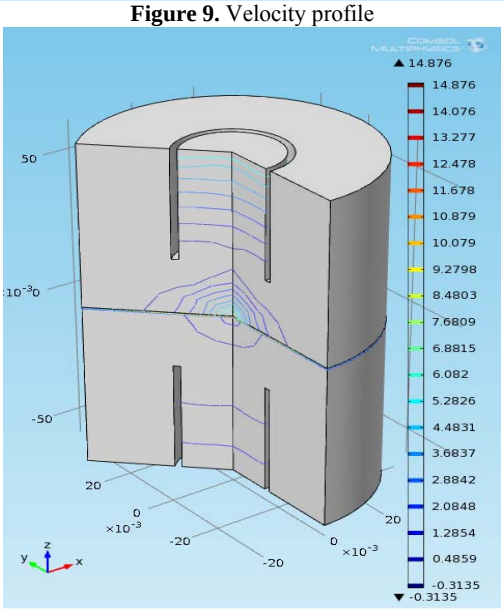

Figure 10. Pressure gradient profile

Figures 11, 12 and 13, finally show the polarization curves obtained from the parametric study: some operating variables have been changed, the cell radius, the temperature and the anode thickness, to see their influence on the cell performance. The increase of the cell radius and the anode thickness have a negative influence on the performance of the cell, in contrast to the temperature, whose increase leads to an improvement of the performance.

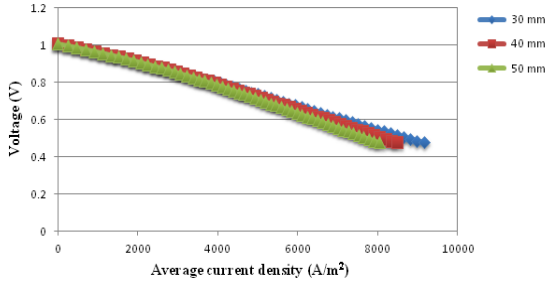

Figure 11. Influence of the cell radius on the polarization curve

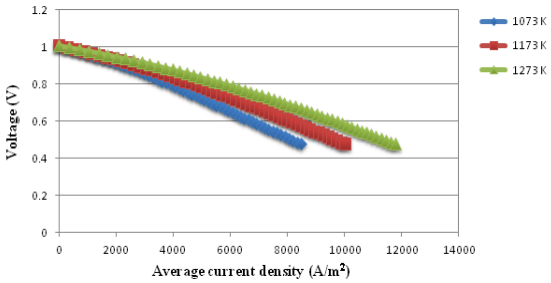

Figure 12. Influence of the temperature on the polarization curve

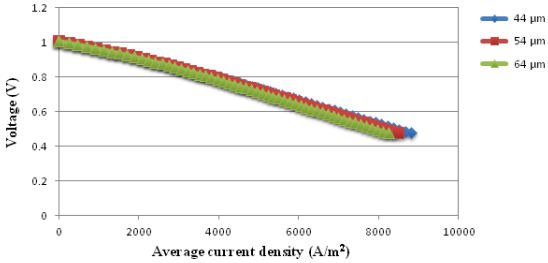

Figure 13. Influence of the anode thickness on the polarization curve

6. Conclusion

A model of Solid Oxide Fuel Cell was first compiled and then analyzed via COMSOL, comparing the results with experimental data: the

similarity between the results has ensured the effectiveness of the model. It was then carried out a parametric study to see the influence of parameters on the model, highlighting its versatility. Future studies, including the temperature profile, will be able to expand this model.

7. References

1. Fergus J. W., Hui R., Li X., Wilkinson D. W., Zhang J., Solid oxide fuel cells: materials properties and performance, CRC Press, 2008
2. Millington R. J., Quirk J. M., Permeability of porous solids, Transactions of the Faraday Society, **vol. 57**, pp. 1200-1207, 1961
3. Singhal S. C., Kendall K., High temperature solid oxide fuel cells: fundamentals, design and applications, Elsevier, 2003
4. Bove R., Ubertini S., Modeling solid oxide fuel cells: methods, procedures and techniques, Springer, 2008
5. Costamagna P., Selimovic A., Del Borghi M., Agnew G., Electrochemical model of the integrated planar solid oxide fuel cell (IP-SOFC), Chemical Engineering Journal, **vol. 102**, pp. 61-69, 2004
6. Janardhanan V. M., Deutschmann O., CFD analysis of a solid oxide fuel fell with internal reforming: coupled interactions of transport, heterogeneous catalysis and electrochemical processes, Journal of Power Sources, **vol. 162**, pp. 1192-1202, 2006
7. Lanzini A., Leone P., Asinari P., Microstructural characterization of solid oxide fuel cell electrodes by image analysis technique, Journal of Power Sources, **vol. 194**, pp. 408-422, 2009
8. Shi Y., Cai N., Li C., Numerical modeling of an anode-supported SOFC button cell considering anode surface reaction, Journal of Power Sources, **vol. 164**, pp. 639-648, 2007
9. Xie Y., Xue X., Multi-scale electrochemical reaction anode model for solid oxide fuel cells, Journal of Power Sources, **vol. 209**, pp. 81-89, 2012
10. Bear J., Dynamics of fluids in porous media, Elsevier Scientific Publishing, 1972
11. Bird R. B., Stewart W. E., Lightfoot E. N., Transport phenomena, John Wiley & Sons, 2005
12. Curtiss C. F., Bird R. B., Multicomponent diffusion, Industrial & Engineering Chemistry Research, **vol. 38**, pp. 2515-2522, 1999
13. Kee R. J., Coltrin M. E., Glarborg P., Chemically reacting flow, John Wiley & Sons, 2003
14. Santarelli M., private communication

8. Appendix

Table.1 Material properties and operating conditions used in this simulation [5,6,8,9]

Operating pressure (Pa)	101325
Inlet temperature (K)	1073
Faraday Constant (C/mol)	96500
Gas constant (J/mol. K)	8.314
Anode ionic conductivity (S/m)	$3.34*10^4$ exp (-10300/*T*)
Cathode ionic conductivity (S/m)	$3.34*10^4$ exp (-10300/*T*)
Anode electronic conductivity (S/m)	$2*10^6$
Cathode electronic conductivity (S/m)	$42*10^4$ exp (-1150/*T*)/T
Electrolyte ionic conductivity (S/m)	$3.34*10^4$ exp (-10300/*T*)
Porosity (ε)	0.4
Particle diameter (m)	$2*10^{-6}$
Tortuosity	$((3-\varepsilon)/2)^{0.5}$
Permeability	$\varepsilon^3 d^2/150(1-\varepsilon)^2$
Inlet velocity (m/s)	0.1
Viscosity of H2 (Pa*s)	$9.27*10^{-6}$
Viscosity of O2 (Pa*s)	$16.27*10^{-6}$
Anode exchange current density (A/m^2)	5300
Cathode exchange current density (A/m^2)	2000
Specific surface area (1/m)	$1.025*10^5$